Let $f^0 = f\ (c_1 = 0, c_2 = 0,\ \chi = 1/2,\ a = a(0))$ denote the free energy per molecule in the planar symmetric bilayer. We assume that this is the equilibrium state of the membrane, an assumption which may be removed later on. Consider now a small bending deformation in which the mid-plane area $A(0) = Na(0)$ remains constant. This defines the mid-plane as the 'surface of in-extension' (or the neutral surface). Let

$$\delta f = f\big(c_1, c_2, 1/2, a(0)\big) - f(0, 0, 1/2, a(0))$$

denote the free energy change associated with the deformation. Transforming, for convenience, from c_1, c_2 to the 'sum' and 'difference' curvatures $c_+ = c_1 + c_2,\ c_- = c_1 - c_2$, we find that, to second order in $c_+,\ c_-$ and χ, the free energy change (per unit area) can be expressed in the form

$$\frac{1}{a(0)}\,\delta f = \frac{1}{2}\,\kappa_b c_+^2 + \frac{1}{4}\,\bar{\kappa}\big(c_+^2 - c_-^2\big) + \frac{1}{2}\,\lambda\Big(\chi - \frac{1}{2}\Big)^2 + \omega\Big(\chi - \frac{1}{2}\Big)c_+. \tag{32}$$

The expansion coefficients, representing elastic moduli of the membrane are determined by the appropriate second derivatives of δf, see below. The curvatures appearing in (32) are measured at the mid-plane. Since δf is symmetric with respect to $c_1, c_2 \to c_2, c_1$ $(c_- \to -c_-)$ the expansion cannot contain a linear (or any odd) term in c_-.

The choice of the mid-plane as the neutral surface, allows to express the free energy change associated with an arbitrary curvature-area deformation as a sum of a stretching term of the form (23), and a bending term of the form (32), without a 'mixed term' $\sim (a - a(0))(c_1 + c_2)$. The choice of the neutral surface enters, implicitly, into the definition of the elastic constants. The coupling between stretching and bending elasticities of membranes is a rather intricate issue involving, apart from the choice of the neutral surface (or surfaces), a careful specification of the conditions under which the deformation takes place [15–19, 92–96].

The constant λ appearing in the third term of (32) is closely related to the area compressibility modulus κ_A defined in (22). This follows from the fact that a change in χ at constant area and curvature, corresponds to changing the head group areas in the two monolayers. A simple relationship between κ_A and λ can be derived if the bilayer is treated as two independent monolayers: For $c_1 = c_2 = 0$, we have

$$\chi = \chi_A = a(0)/2a_A, \qquad \chi_B = 1 - \chi = a(0)/2a_B,$$

cf. (27). Thus,

$$\delta\chi = (\chi - 1/2) = -\big[a(0)/2a_A^2\big]\delta a_A = -(1/2)(\delta a/a_0)$$

since at equilibrium $a_A = a(0) = a_0$. Thus, comparing the expressions for δf obtained using (23) and (32), we find

$$\lambda \simeq 4a_0\kappa_A. \tag{33}$$

measured by χ, may be coupled to the change in the bilayer curvature. A change in χ in the course of a curvature fluctuation may be due to lateral diffusion of molecules within each monolayer (into and out of the section of bilayer under discussion). Another, much less likely, mechanism on the time scale of membrane fluctuations, is a 'flip-flop' exchange between the monolayers [15–19]. There are cases, e.g., when the hydrophilic head groups are chemically polymerized, that the exchange is 'blocked' and χ is a constant, independent of c_1, c_2. The opposite limit of 'free exchange' corresponds to the case where χ adjusts freely to the momentary curvatures so as to minimize δf. Thus, generally, one can treat χ as a function of c_1 and c_2, which to first order in c_1, c_2 is a function of $c_+ = c_1 + c_2$ since

$$\chi - \frac{1}{2} = \left(\frac{\partial \chi}{\partial c_1}\right)_{0,0} c_1 + \left(\frac{\partial \chi}{\partial c_2}\right)_{0,0} c_2 = \left(\frac{\partial \chi}{\partial c_+}\right)_{0,0} c_+ = \eta d c_+ \tag{34}$$

with the derivative evaluated at the planar geometry, and with the second equality serving as the definition of η. (In passing to the second equality we made use of the fact that for a laterally isotropic bilayer $(\partial\chi/\partial c_1) = (\partial\chi/\partial c_2) = (\partial\chi/\partial c_+)$.) η is a dimensionless concentration-composition coupling parameter which depends on the mode of deformation.

Using (34) we rewrite (32) in the form

$$\frac{1}{a(0)}\,\delta f = \frac{1}{2}\,\kappa c_+^2 + \frac{1}{4}\,\bar{\kappa}\left(c_+^2 - c_-^2\right) \tag{35}$$

with the rescaled bending constant

$$\kappa = \kappa_b + \omega d\eta + \frac{1}{2}\,\lambda d^2 \eta^2. \tag{36}$$

The special case of 'blocked exchange' corresponds to $\eta = 0$, cf. (34), and hence $\kappa = \kappa_b$. The minimum value of κ as a function of η, corresponding to 'free exchange', is obtained when $\eta = -\omega/\lambda d$, in which case

$$\kappa = \kappa_b - \omega^2/2\lambda. \tag{37}$$

A third special case of interest corresponds to a bending deformation during which the areas per head group, at both interfaces, remain constant $a_A = a_B = a(0)$. In this case, $\delta f \simeq \delta f_t$ is due, almost entirely, to ('splay-like') chain conformational distortion. Using (27) we see that, to first order, $a_A = a(0)$ implies $\chi - 1/2 = dc_+/4$, corresponding to $\eta = 1/4$ in (34).

A more general form of the deformation free energy, allowing for the case that the planar bilayer is not the equilibrium geometry (but still serving as a reference state)

obtain

$$\frac{1}{a(0)}\,\delta f = \frac{1}{2}\,\kappa(c_+ - c_0)^2 + \frac{1}{4}\,\bar{\kappa}\left(c_+^2 - c_-^2\right) - \frac{1}{2}\,\kappa c_0^2$$
$$= \frac{1}{2}\,\kappa\left(c_1 + c_2 - c_0\right)^2 + \bar{\kappa} c_1 c_2 - \frac{1}{2}\,\kappa c_0^2 \tag{38}$$

with the second equality expressing the familiar Helfrich form [15–19]. The last term ensures that $\delta f = 0$ for the planar bilayer. Note that the χ dependence of δf is absorbed into κ. The constants $\kappa, \bar{\kappa}$ and c_0 are the familiar splay modulus, saddle splay modulus and the spontaneous curvature [15–21]. As is well known, and easy to show, the equilibrium curvatures are given by

$$c^{\mathrm{eq}} = c_1^{\mathrm{eq}} = c_2^{\mathrm{eq}} = c_+^{\mathrm{eq}}/2 = \kappa c_0/(2\kappa + \bar{\kappa}), \qquad c_-^{\mathrm{eq}} = 0.$$

Thus, $c^{\mathrm{eq}} = c_0 = 0$ is the equilibrium condition for the planar bilayer. Thermodynamic stability requires that $\kappa > -\bar{\kappa}/2 > 0$.

From (38) it follows immediately that

$$\kappa = \frac{1}{a(0)}\left\{\left(\frac{\partial^2 f}{\partial c_+^2}\right) + \left(\frac{\partial^2 f}{\partial c_-^2}\right)\right\}, \tag{39}$$

$$\bar{\kappa} = -\frac{2}{a(0)}\left(\frac{\partial^2 f}{\partial c_-^2}\right), \tag{40}$$

$$\kappa c_0 = -\frac{1}{a(0)}\left(\frac{\partial f}{\partial c_+}\right) = \frac{1}{a(0)}\,c_+^{\mathrm{eq}}\left(\frac{\partial^2 f}{\partial c_+^2}\right) \tag{41}$$

with all derivatives evaluated at the planar geometry, $c_+ = c_- = 0$ ($c_1 = c_2 = 0$). Notice that $f = f(c_+, c_-)$ is treated here as a function of c_+ and c_- only; the χ dependence has been absorbed into f through (34).

3.2.3. Molecular theory

Application of the general thermodynamic relations (39)–(41) to the tail free energy f_{t}, as given by (30), yields explicit expressions for the chain contribution to the curvature elastic constants. After some algebra, involving the use of (11) for Ω_{A} and Ω_{B} and of the packing constraint (31), one finds [37]

$$\kappa c_0 = \int \pi(z) z \,\mathrm{d}z, \tag{42}$$

$$\bar{\kappa} = -\int \pi(z) z^2 \,\mathrm{d}z \tag{43}$$

the tails contribution to the elastic constants (which is the contribution explicitly considered here) comes from $-d/2 \leqslant z \leqslant d/2$. By extending the integrals to the aqueous regions one obtains also the interfacial (head group repulsion and surface tension) contributions to the κc_0 and $\bar{\kappa}$ (see below). Similarly so for the integrals appearing in the expressions for κ as outlined next.

The expression obtained for κ (using (39) and (30)) involves three terms[37]:

$$\begin{aligned}\kappa = &-\int \left(\frac{\partial \pi}{\partial c_+}\right)_\chi z\,\mathrm{d}z - \frac{1}{2}\eta d \int \left(\frac{\partial \pi}{\partial \chi}\right) z\,\mathrm{d}z \\ &+ \frac{1}{16}\,\frac{\eta^2 d^2}{a(0)} \int \left(\frac{\partial \pi}{\partial \chi}\right)\left[\langle \phi_{\mathrm{A}}(z)\rangle - \langle \phi_{\mathrm{B}}(z)\rangle\right] \mathrm{d}z\end{aligned} \tag{44}$$

with all derivatives evaluated at the planar geometry, $c_+, c_- = 0$, and it should be noted that the derivative appearing in the first integrand is evaluated for a bilayer with constant 'composition' χ. The three terms in (44) correspond, respectively, to the three terms in (36). The first and third terms, representing κ_{b} and $\lambda d^2\eta^2/2$ are positive, while the second ('coupling') term is negative. This follows from the fact that upon increasing c_+ (at constant χ) the area per molecule increases for $z > 0$ and decreases for $z < 0$, implying that $(\partial\pi/\partial c_+)_\chi$ is negative at $z > 0$ and positive at $z < 0$. Similarly, upon increasing $\chi = \chi_{\mathrm{A}}$ at constant curvature ($c_+ = c_- = 0$) the area per molecule decreases ($\pi(z)$ increases) in the upper monolayer ($z > 0$), and increases (lower $\pi(z)$) in the lower monolayer. Thus the second integral in (44) is obviously positive. The third is positive because $\langle \phi_{\mathrm{A}}(z)\rangle - \langle \phi_{\mathrm{B}}(z)\rangle$ is positive at $z > 0$ and negative at $z < 0$. It should be noted that $\bar{\kappa}$, unlike κ, is independent of η, i.e. independent of the mode of deformation [37].

Analogous expressions to (42) and (43), with $\sigma(z) = -\pi(z)$, representing the stress profile in the bilayer, have originally been derived by Helfrich based on thermodynamic-mechanical considerations [17]. (Equation (44) was derived in [37] and a similar expression in [97].) In Helfrich's expressions the integrations extend from $-\infty$ to $+\infty$ and thus include the contributions to the elastic constants arising from the interactions prevailing in the interfacial region, $f_{\mathrm{h}} + f_{\mathrm{s}}$ in our notation. The integration limits in (42)–(44) can be extended similarly, provided we interpret $\pi(z) = \pi_{\mathrm{t}}(z) + \pi_{\mathrm{s}}(z) + \pi_{\mathrm{h}}(z)$ as a sum of tail, surface tension and head group terms [19]. $\pi_{\mathrm{t}}(z)$, defined between $-d/2$ and $+d/2$, is the chain lateral pressure appearing in (10) and (11). For f_{s}, using again the simple form (3) we should set

$$\pi(z) = -\gamma a_{\mathrm{A}}\delta(z - d/2) - \gamma a_{\mathrm{B}}\delta(z + d/2),$$

with a_{A} and a_{B} given by (27). Similarly, the simple model (4) for f_{h} implies

$$\pi_{\mathrm{h}}(z) = \left(C/\tilde{a}_{\mathrm{A}}^2\right)\delta(z - d/2 - \tilde{\delta}) + \left(C/\tilde{a}_{\mathrm{B}}^2\right)\delta(z + d/2 + \tilde{\delta}),$$

interface; $\tilde{a}_A$ is given by (27) with d replaced by $d/2 + \tilde{\delta}$.

Although we have so far been explicitly concerned with single-component and symmetric ($\chi = 1/2$) bilayers, it should be noted that (42)–(44) apply just as well to mixed and/or non-symmetric systems. The composition and concentration dependencies of κ, $\bar{\kappa}$ and c_0 enter through the $\pi(z)$ profile. The lateral pressure $\pi(z)$, in turn, is dictated by packing conditions of the form (31) which can easily be extended to mixed bilayers. The only assumptions here are that the compositions (but not necessarily the head group areas) and the (random) lateral distributions in each monolayer are not allowed to vary in the course of a curvature deformation. Including these variables as additional degrees of freedom (thus also allowing for lateral segregation in each leaflet), would result in additional terms in (44).

From (42) we see immediately that for a symmetric bilayer, where $\pi(z) = \pi(-z)$, the equilibrium curvatures are $c_+^{eq} = c_-^{eq} = c_0 = 0$, as expected. Using (43) one can evaluate the saddle-splay constant, $\bar{\kappa}$, using the lateral pressure profile $\pi(z)$ of the planar bilayer. Numerical calculations of $\bar{\kappa}_t$, the chain contributions to $\bar{\kappa}$, reveal that it is negative [37]. Its magnitude, $|\bar{\kappa}_t|$, increases moderately (roughly linearly) with chain length, n, and decreases very steeply ($\sim a^{-b}$ with $b \sim 10$) as the area per chain, a, increases (lower $\pi(z)$). Typical values of $|\bar{\kappa}_t|$, e.g., when $a \simeq 30$ Å^2, range from $\sim 3kT$ for $n = 8$ to $\sim 20kT$ for $n = 16$. In a mixed bilayer of, say, C_8 and C_{16} chains, $\bar{\kappa}_t$ varies roughly linearly with composition. The surface tension contribution to $\bar{\kappa}$ can be estimated using (29). From (29) and (38) we get $\bar{\kappa}_s = \gamma d^2/8 = \gamma\nu^2(n/a)^2/4$. (At equilibrium, as noted in section 3.1, $a \sim n^g$, hence $\bar{\kappa}_s \sim n^{2-g}$, with g ranging between 0 and 1/3.) For $n \simeq 16$, $a \simeq 30$ Å^2 and $\gamma \simeq 0.1kT/$Å^2 one finds $d \simeq 30$ Å and thus $\bar{\kappa}_s \sim 10kT$, comparable but smaller than $-\bar{\kappa}_t$. Ignoring $\bar{\kappa}_h$, one finds $\bar{\kappa} = \bar{\kappa}_t + \bar{\kappa}_s \sim -10kT$. As noted above, $-\bar{\kappa}$ is expected to decrease steeply as a increases. Under certain conditions $\bar{\kappa}$ may become positive, violating the bilayer stability condition and favoring spontaneous saddle-like structures [20, 21, 92–94]. It should be noted, however, that all model calculations of $\bar{\kappa}$ reported so far, including the above, involve considerable uncertainties, reflecting the high sensitivity of the results to the details of the molecular model used (especially for head group interactions [19, 84]). The estimates of the splay bending constant, κ, or more precisely its tail component κ_t seem more reliable.

The bending modulus, κ, can be calculated using (46). The curvature and concentration derivatives of $\pi(z)$ appearing in this equation can be evaluated by solving (numerically) a set of integral equations containing these derivatives, which are obtained by differentiation of the packing constraint (1.31). Additional details are given in [37].

Figures 5 and 6, both taken from the work of Szleifer et al. [37], show two sets of calculated (chain part, κ_t of) κ for three types of bending deformations. Figure 5 demonstrates, for a pure bilayer composed of C_{16} chains, how κ varies with the average area per chain, $a(0)$ (= a in the planar geometry) for the three modes of bending deformations mentioned in connection with (36): a) 'Blocked exchange', corresponding to $\eta = 0$ in (36) and (44), in which case $\chi = 1/2$ is constant and $\kappa = \kappa_b$ is maximal, since no concentration relaxation (e.g., via lateral diffusion)

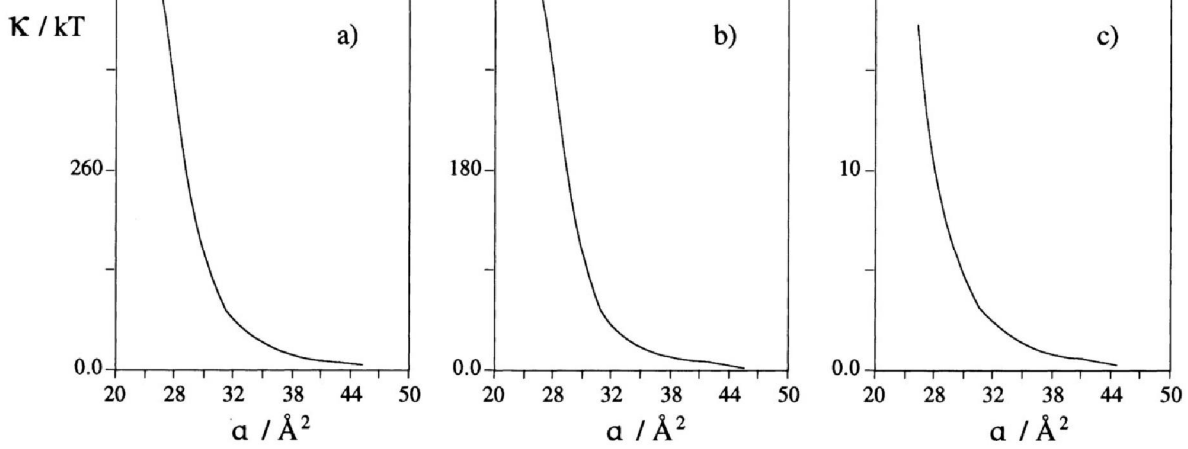

Fig. 5. The chain part of the bending modulus as a function of the average area per chain (in the planar bilayer). a), b) and c) correspond to: blocked exchange, constant area and free exchange deformations, respectively [37] (see text).

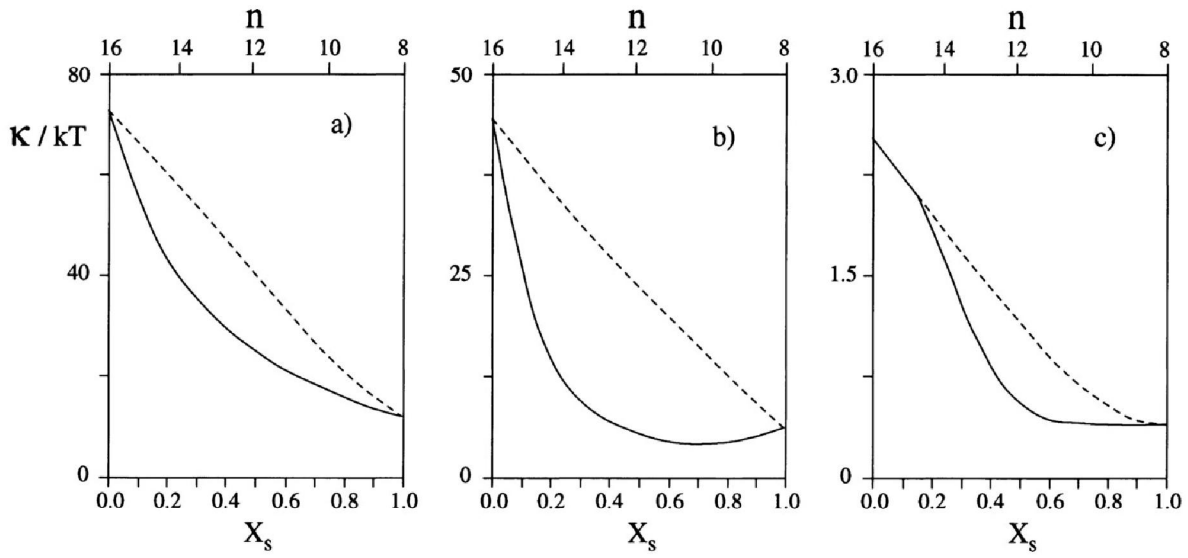

Fig. 6. The chain part of the bending modulus as a function of chain length (dashed lines, upper scale), and as a function of the short chain fraction X_s in a mixed bilayer of C_8 and C_{16} chains (full lines, lower scale) [37]. The three cases considered are the same as in fig. 5 (see text).

accompanies the bending deformation; b) 'Constant area' deformation. In this case χ changes in the course of the deformation, ensuring that $a_A = a_B = a(0)$ stays constant at all curvatures. As noted earlier this deformation mode corresponds to $\eta = 1/4$. Physically this special case is characteristic of a bilayer in which the equilibrium area per head group is fully governed by the balance between head group repulsion and surface tension (i.e. by π_h and π_s in (21), implying $a_0 = a_h$), with the chains adjusting to the area prescribed by the interfacial interactions. c) 'Free exchange', in which case χ adjusts freely at each curvature, so as to minimize κ (more precisely, κ_t). Here $\kappa = \kappa_b - \omega^2/2\lambda$, cf. (37). In all cases κ increases steeply as a decreases (below $a \approx 30$ Å^2), reflecting the strong increase in the magnitude of the

approximate scaling argument, explaining qualitatively the a and n dependence of κ is given below). For typical values of the area per chain in phospholipid bilayers, $a \sim 30-35$ Å^2 ($\sim 60-70$ Å^2 per head group of doubly chained lipids), the results in fig. 5 show that for C_{16} chains κ_t varies between $\sim 70kT$ in case (a) to $\sim 3kT$ in case (c). These estimates should be regarded as lower bounds to κ, since the calculations do not include κ_h – the head group contribution to κ. (The surface term, at least according to (29), is negligible.) Estimates of κ_h, based on electrostatic or excluded volume interaction models, are typically on the order of few kT, or less [81–85]. For bilayers composed of (or containing) short chains (see below), or at relatively large head group areas, this contribution to κ can be most significant, especially in the case of free exchange. Typical experimental values of κ for phospholipid bilayers are $\sim$ 10–50kT, [15–19, 22–27]. Considerably smaller bending constants, $\kappa \sim 1kT$, were measured for bilayers containing short chain amphiphiles [28, 29], or 'bola' lipids [25–27]. A possible explanation of these observations is provided by chain packing considerations, as outlined next.

Figure 6 displays the variation of $\kappa = \kappa_t$ with the amphiphile chain length ($n = 8$–16), for a fixed value of the average area per chain in the planar bilayer, $a = 31.6$ Å^2. Also shown in this figure is the dependence of κ on the mole fraction of short chains in a binary bilayer of randomly mixed C_{16} and C_8 chains. In the latter calculation the composition (C_8/C_{16} ratio) is the same in both monolayers, and is not allowed to change as a function of curvature. As in fig. 5, the three modes of deformation considered are: a) Blocked exchange; b) Constant area, and c) Free exchange. In all cases corresponding to the single-component bilayers, κ rapidly decreases with n, approximately according to $\kappa \sim n^\alpha$ ($\alpha \simeq 3$), reflecting mainly the increase with n in the range ($-d/2 \leqslant z \leqslant d/2$) over which $\pi(z) > 0$. The addition of small amounts of short chains (C_8) to a bilayer composed of longer chains (C_{16}) leads to a more dramatic lowering of κ, in qualitative agreement with experiment [25–29]. This behavior reflects the substantial decrease of $\pi(z)$, or more precisely of the range over which $\pi(z)$ is large, attendant upon the addition of short chains to the membrane, as illustrated schematically in fig. 7. The addition of short chains of, say, n_s segments relieves much of the lateral stress on the last $\sim n_l - n_s$ segments of the long chains, i.e. those which need not compete for the available volume with the short chains.

The conclusions derived from fig. 5 regarding the n and χ dependence of κ should be subjected to the assumption that $a(0) = a$ is the same in all cases considered. However, this is not necessarily the equilibrium area per chain a_0 (in the planar bilayer) for all cases. Although we have concluded that a_0 varies only weakly with n, this dependence may be amplified in κ due to the strong dependence of κ on a, cf. fig. 5. Suppose $\kappa \sim n^\alpha/a^\beta$ and $a_0 \sim n^g$ then, at a_0, $\kappa \sim n^\gamma$ with $\gamma = \alpha - \beta g$. A simple model, outlined below, suggests $\alpha \simeq 3$ and $\beta \simeq 5$ (the numerical calculations suggest $\beta \simeq 7$ [37]). We have concluded earlier that g varies between 0 and 1/3, hence γ may be as low as 4/3 (or even 2/3 if one uses $\beta = 7$) if $g = 1/3$, i.e. if a_0 is determined only by the balance between chain repulsion and surface tension while head group repulsion is negligible. In this case the lowering of κ by the addition of

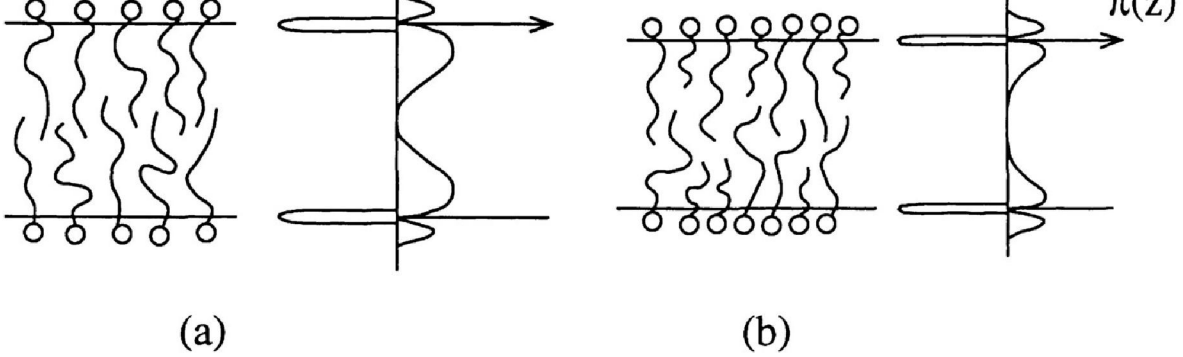

Fig. 7. Schematic illustration of the lateral pressure profile in a single component bilayer (left), and a mixed bilayer of short and long chains. Note the decrease in the bilayer thickness, and the decrease in the tail contribution to $\pi(z)$.

short chains is also expected to be less dramatic. Indeed, recent calculations of κ for a monolayer of diblock copolymers (where only chain repulsion is relevant) suggest that for a mixture of symmetric diblock chains κ varies approximately linearly with composition [98].

We close this section with an approximate scaling argument which, based on a simple 'compressional model' [36, 99], can explain qualitatively why and how κ increases with n and decreases with a. Consider a cylindrical deformation ($c_1 = c$, $c_2 = 0$) of a symmetric planar bilayer, with $a(0) = a_0$ denoting the average area per head group in the planar geometry. From (39), for this deformation, $\kappa = (1/a_0)(\partial^2 f/\partial c^2)$. Suppose for concreteness that the bending takes place under the condition of blocked exchange. Upon bending the bilayer, the average area per head group in the 'outer' (convex, A) monolayer changes from a_0 to

$$a_A = a_0(1 + cd/2) = a_0(1 + cl_0).$$

Similarly,

$$a_B = a_0(1 - cd/2) = a_0(1 - cl_0)$$

with $d/2 = l_0 = v/a_0 \sim n/a_0$ denoting the average chain length in the planar bilayer. As in section 3.1, let $l_c \sim n^{1/2}$ denote the average length of the 'free'(unstretched) chain. Then, $f \sim (l_0/l_c)^2$ is the free energy per chain in the planar geometry ($f = f_t$). In the curved geometry the average chain lengths are given by

$$l_A = l_0 a_0/a_A \cong l_0(1 - cl_0)$$

and

$$l_B = l_0 a_0/a_B \cong l_0(1 + cl_0).$$

$$\delta f = (\delta f_A + \delta f_B)/2 \sim [(l_A/l_c)^2 + (l_B/l_c)^2 - 2(l_0/l_c)^2]$$
$$= (l_0/l_c)^2 l_0^2 c^2 \sim (n^3/a_0^4)c^2.$$

Hence (the tail part of) the bending constant is

$$\kappa = (1/a_0)(\partial^2 f/\partial c^2) \sim n^3/a_0^5.$$

The arguments given above are obviously rather crude since a bending (splay) deformation involves a change in the average shape of the chain (from a 'cylinder' to a 'truncated cone') and not only in its average cross sectional area. Notwithstanding this proviso, the approximate model can be used to derive a simple relationship between κ and the area compressibility modulus κ_A defined in (23), (hence the term 'compressional model'). For the cylindrical deformation,

$$\delta a_A = a_A - a_0 = a_0 c l_0$$

and

$$\delta a_B = a_B - a_0 = -a_0 c l_0.$$

Now, using (23) for each of the two monolayers, and noting $2\kappa_A$ (monolayer) = κ_A (bilayer) we find

$$\delta f = (\delta f_A + \delta f_B) = \kappa_A a_0 l_0^2 c^2/2 = \kappa a_0 c^2/2$$

with the last equality expressing the bending energy for cylindrical deformation. We thus find $\kappa_A \sim \kappa/l_0^2$ and hence $\kappa_A \sim n/a_0^3$ since $l_0 = v/a_0 \sim n/a_0$.

4. Lipid-protein interaction

The presence of a rigid hydrophobic solute, such as an integral protein or a cholesterol molecule in the membrane, introduces additional boundary conditions on its lipid environment – beyond the usual packing constraints prevailing in the 'unperturbed' (solute-free) membrane. The rigid solute, say the hydrophobic part of a trans-membrane protein, restricts the conformational freedom (entropy) of the lipid chains surrounding it. Furthermore, if the hydrophobic thickness of the protein, d_P, is different from that of the lipid bilayer, d_L^0, then neighboring lipid chains should stretch out (if $d_P > d_L^0$) or compress (if $d_P < d_L^0$), in order to minimize the contact area between hydrophobic groups and the surrounding aqueous solution. These and other factors, such as the detailed shape of the protein, differences between the 'hydrophobicity' of the lipid chains and the protein amino acid residues, and the

the nature and the extent of the lipid-protein interaction free energy.

The importance of lipid-protein interactions in controlling the biological activity of certain membranal proteins and in modifying the physico-chemical properties of biological membranes [41, 47, 100–102] has motivated the development of many theoretical models of these phenomena [40–60]. Some of these models are based on Landau-type expansions of the interaction free energy, with the '*hydrophobic mismatch*', $d_P - d_L^0$, or related quantities serving as the thermodynamic order parameters in the free energy expansion [40, 41, 43–46]. Other authors have formulated continuum models, of the kind used in the elastic theory of (smectic) liquid crystals, representing the influence of the protein [54–56] by additional boundary conditions. There are also some computer simulation studies [57–59]. Only a few theoretical studies have addressed the issues of lipid-protein and lipid mediated protein-protein interactions from a molecular, statistical thermodynamic, approach. The latter include the seminal, mean-field, approach developed by Marčelja (for the case $d_P = d_L^0$) [42], Pink's 'ten-state model' [48] and the 'mattress model' of Mouritsen, Bloom and coworkers [41, 50, 51] which has been extensively applied to a variety of issues, notably to investigate the role of the hydrophobic mismatch in membrane phase transitions. Several comprehensive reviews of the theoretical approaches to lipid-protein interaction are available [40, 41, 100], and there is no reason to repeat their analysis here. Thus, in this section we focus attention on one very recent and rather simple model [60] constituting a natural extension and application of the concepts developed in the previous sections.

4.1. The model

As in most previous models of lipid-protein interaction the protein is treated in this model as a smooth and rigid solute embedded in the bilayer hydrophobic core, as illustrated schematically in fig. 8. For concreteness, the hydrophobic part of the protein may be envisioned as a cylinder of height d_P and radius $\mathcal{R} \gg a_0^{1/2}$, with a_0 denoting the average area per chain in the unperturbed bilayer. Thus, to the lipid chains surrounding it, the protein presents an essentially flat and impenetrable wall. The protein and the lipid chains are assumed to have similar hydrophobicities, so that lipid-lipid and lipid-protein attractions are the same. Interactions between the lipids polar heads and hydrophilic groups of the protein are not included in the model. Consequently, the lipid-protein interaction free energy is due entirely to the boundary conditions on lipid conformational freedom imposed by the protein wall, and (when $d_P \neq d_L^0$), to the elastic deformations of lipid chains associated with the adjustment of the bilayer thickness to that of the protein.

Let $d_L(x)$ denote the bilayer hydrophobic thickness at distances x from the protein. The condition of hydrophobic matching at the lipid-protein interface requires $d_L\ (x = 0) = d_P$, see fig. 8. The decay of $d_L(x)$ to the unperturbed bilayer thickness, $d_L\ (x \to \infty) = d_L^0$, is assumed to be exponential

$$d_L(x) = d_L^0 + (d_P - d_L^0) \exp(-x/\xi) \tag{45}$$

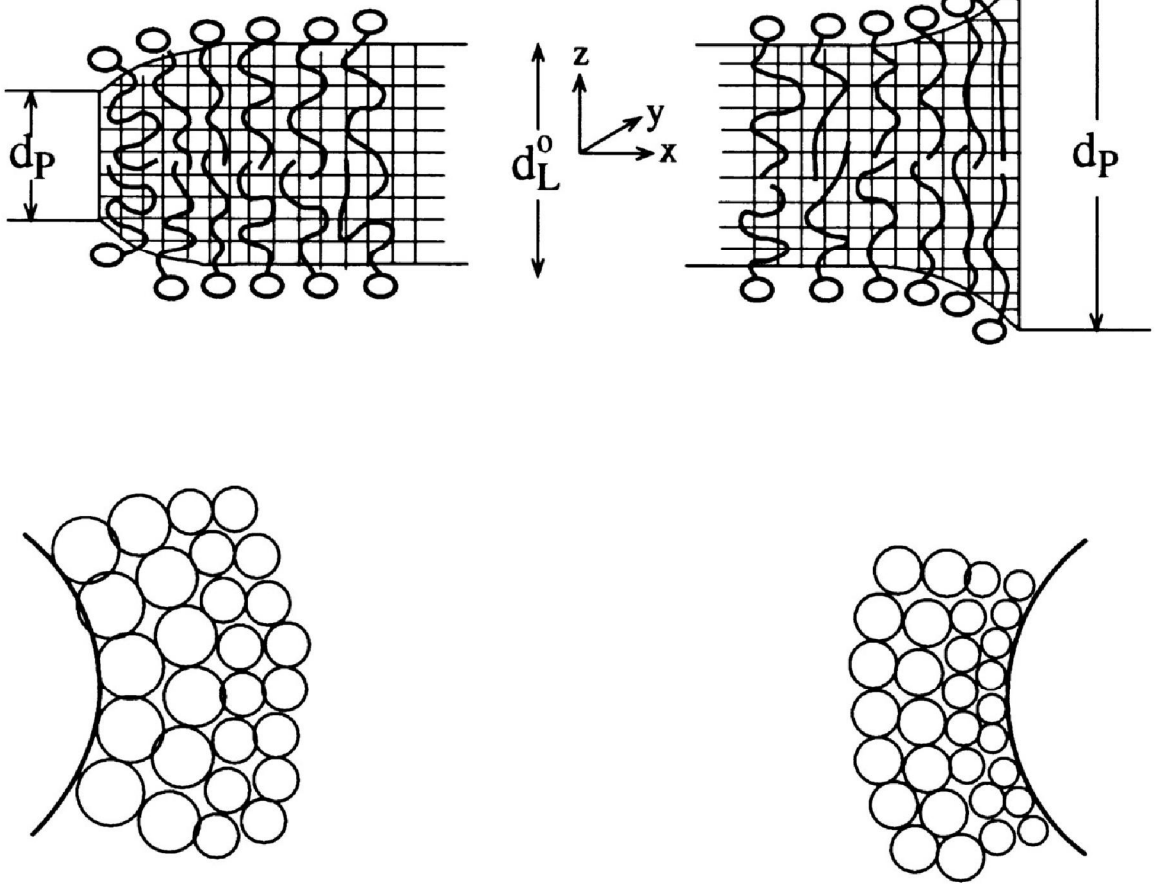

Fig. 8. Schematic illustration of the lipid-protein interaction model. Negative hydrophobic mismatch (left) results in bilayer compression and hence an increase in the average area per lipid head group near the protein. Positive mismatch results in chain stretching in the vicinity of the protein [60].

with ξ denoting the 'coherence length' of the perturbation. (The range of the perturbation is $\sim 3\xi$.) The model treats ξ as a variational parameter, determined by minimization of the lipid-protein interaction free energy ΔF. The exponential form (45) is predicted by the phenomenological (Landau-type) models of lipid-protein interaction. It should be mentioned, however, that other functional forms for $d_L(x)$ have been inferred by other approaches [53–56]. The model described here is not capable of predicting the analytic form of $d_L(x)$, so that (45) should be regarded as a convenient reasonable parametrization.

Unlike the case of uniform bilayers, the presence of the protein implies that lipid molecules anchored at different distances from the protein are characterized by different conformational properties and, when $d_P - d_L^0 \neq 0$, by different head group densities. Accordingly, the free energy per molecule,

$$f(x) = f_t(x) + f_h(x) + f_s(x) \tag{46}$$

is now a function of x. The three terms on the right hand side of (46) describe, as in (1), the tail, head and surface contributions to f.

wall) and length L along the x direction; both L_y and L_x are taken to be large on a molecular scale, say $L_y \gg a^{1/2}$ and $L_x \gg \xi$. (As we shall see below, ξ is typically of the order of several molecular diameters, i.e. ξ is several times larger than $a^{1/2}$). Let $dN_A = \sigma_A(x)L_y\,dx$ denote the number of chains anchored to the upper, A, interface, within the distance interval $x, x + dx$. $dN_B = \sigma_B(x)L_y\,dx$ is the number of chains originating, within the same interval, from the lower interface. Using $dV(x) = d_L(x)L_y\,dx$ to denote the volume of the membrane 'slice' $L_y\,dx$, we find $\sigma_B(x)+\sigma_A(x) = d_L(x)/v$, with v denoting the volume per chain. In a symmetric bilayer,

$$\sigma_A(x) = \sigma_B(x) = \sigma(x) = d_L(x)/2v.$$

For $x \gg \xi$, $\sigma(x) \to \sigma_0 = d_L^0/2v = 1/a_0$. Note however that, whenever $d_L^0 \neq d_P$ the interface is curved and, for small x, $\sigma(x) \neq 1/a(x)$, where $a(x)$ is the local head group area, see below.

The free energy of the lipids in the above slab, per unit length of the protein wall (i.e. the free energy divided by L_y) is given by

$$F = \int \left[\sigma_A(x)f_A(x) + \sigma_B(x)f_B(x)\right] dx = 2\int \sigma(x)f(x)\,dx \tag{47}$$

with the second equality holding for symmetric bilayers. Equation (47) can be generalized to the case of mixed lipid bilayers, by adding the contributions of the different molecular species, and by adding a (x dependent) mixing entropy term. This is an interesting case, especially because of the possibility of protein induced lipid demixing, i.e. enhanced concentration of one (or more) species in the vicinity of the protein. However, for the sake of simplicity the following discussion will be limited to symmetric, single component, membranes.

The lipid-protein interaction free energy is defined by

$$\Delta F = F - F^0 = 2\int \sigma(x)\left[f(x) - f^0\right] dx \tag{48}$$

with $f^0 = F^0/2N$ denoting the free energy per molecule in the protein free bilayer; $f^0 = f\ (x \to \infty)$.

By a straightforward generalization of the phenomenological models for f_h and f_s from section 2.1, we obtain

$$f_s(x) + f_h(x) = \gamma a(x) + C/a(x) = \gamma a(x)\left[1 - \frac{a_h}{a(x)}\right]^2 + \text{const} \tag{49}$$

with $C = \gamma a_h^2$. The average local area per head group, at distance x from the protein, is given by

$$a(x) = \frac{2v}{d_L(x)}\left[1 + \left(\frac{d_L'(x)}{2}\right)^2\right]^{1/2} \tag{50}$$

$$d'_{\mathrm{L}}(x) = \left[d_{\mathrm{L}}(x) - d^0_{\mathrm{L}}\right]/\left(d_{\mathrm{P}} - d^0_{\mathrm{L}}\right).$$

The local chain free energy is given by

$$f_{\mathrm{t}}(x) = \sum_{\alpha} P(\alpha; x)\varepsilon(\alpha) + kT \sum_{\alpha} P(\alpha; x) \ln P(\alpha; x) = \varepsilon_{\mathrm{t}}(x) - T s_{\mathrm{t}}(x) \tag{51}$$

with $P(\alpha; x)$ denoting the local singlet distribution of chain conformations. Again, the 'actual' $P(\alpha; x)$ can be determined through minimization of

$$F_{\mathrm{t}} = 2 \int \sigma(x) f_{\mathrm{t}}(x)\, \mathrm{d}x$$

subject to the relevant packing constraints on $\{P(\alpha; x)\}$. In formulating these constraints it should be noted that, unlike the case of an unperturbed bilayer, here the system, and hence the singlet distribution, is not invariant to translations in the xy plane but, rather, only to translation along y.

Let $\rho(\vec{R})$ denote the chain segment density at an arbitrary point $\vec{R} = X, Y, Z$ within the hydrophobic interior of the bilayer. As usual, we assume that the segment density is uniform and liquid-like throughout the hydrophobic core: $\rho(\vec{R}) = \rho = 1/\nu$, where ν is the specific volume per segment in a bulk liquid hydrocarbon. Again, $\rho(\vec{R}) = \rho$ can be expressed in the form of a packing constraint on $\{P(\alpha; x)\}$. It should be noted that the density at $\vec{R}$ involves contributions from all chains, on both interfaces, which are within reach of this point. It is not difficult to show that the appropriate form of the packing constraint for a symmetric bilayer (of width $L_{\mathrm{y}} = 1$ along the y axis) is

$$\int \sigma(x) \sum_{\alpha} P(\alpha; x)\left[\phi_{\mathrm{A}}(\alpha, \vec{S}; x) + \phi_{\mathrm{B}}(\alpha, \vec{S}; x)\right] \mathrm{d}x = \rho \quad (\text{all } \vec{S}). \tag{52}$$

In this equation $\vec{S} = X, Z$ denotes an arbitrary point in the xz plane of the membrane. $\phi_{\mathrm{A}}(\alpha, \vec{S}; x)\, \mathrm{d}S/\nu$ is the number of segments belonging to a chain in conformation α, anchored to the A interface at distance x from the protein, whose X, Z coordinates fall within the small area element $\mathrm{d}X\, \mathrm{d}Z$ around X, Z (regardless of their Y coordinates).

The minimization of F_{t} subject to (52) yields

$$P(\alpha; x) = \frac{1}{\Omega(x)} \exp\left[- \beta\varepsilon(\alpha) - \beta \int \lambda(\vec{S})\phi(\alpha, \vec{S}; x)\, \mathrm{d}\vec{S}\right] \tag{53}$$

with $\{\lambda(\vec{S})\}$ denoting the set of Lagrange parameters conjugate to (52). Their values are determined, as usual, by substitution of (53) into the packing constraints (52) and solving, numerically, the resulting self-consistency equations. The numerical

because the number of equations that need to be solved is bigger: the XZ plane is now divided into many 'boxes' $\Delta X \Delta Z$, rather than into several 'layers' of thickness ΔZ. Second, because the segment density in box $\Delta X \Delta Z$ collects contributions from (non-equivalent) chains originating at several different points x. Nevertheless, these calculations can easily be performed using ordinary work stations.

Using (47) and (51)–(53), one finds

$$F_{\mathrm{t}} = -2kT \int \sigma(x) \ln\, \Omega(x)\, \mathrm{d}x - \rho \int \lambda(\vec{S})\, \mathrm{d}\vec{S}. \tag{54}$$

This, as well as all previous equations in this section reduce to those of the unperturbed bilayer when $P(\alpha; x) = P(\alpha)$ and $\sigma(x) = \sigma$ are independent of x.

4.2. The role of hydrophobic mismatch

As in section 2, the expressions derived in section 4.1 can be used to calculate both single chain (conformational) properties and thermodynamic functions of interest. Some of the qualitative conclusions can easily be explained by reference to fig. 8. For instance, in the immediate neighborhood of the protein the calculated orientational order parameters reveal enhanced orientational order when $d_{\mathrm{P}} > d_{\mathrm{L}}^0$ and a lower degree of orientational order in the case of negative hydrophobic mismatch, $d_{\mathrm{P}} < d_{\mathrm{L}}^0$. This, obviously, is a direct reflection of the enhanced chain stretching in the former case as opposed to chain compression in the latter. These results are consistent with experiment [11]. It has been suggested, based on qualitative theoretical consideration and various experimental observations, that the chains in the vicinity of the protein should show a finite tilt angle of their 'director' (the average end-to-end vector) [10]. The results obtained from calculations based on (53) confirm this prediction revealing also that the tilt angle is small when $d_{\mathrm{P}} > d_{\mathrm{L}}^0$ and relatively large when $d_{\mathrm{P}} < d_{\mathrm{L}}^0$. A finite tilt is also observed when $d_{\mathrm{P}} = d_{\mathrm{L}}^0$, resulting from chain repulsion by the protein wall [60].

Figure 9, taken from the work of D. Fattal [60], shows the results obtained for the lipid-protein interaction free energy as a function of the hydrophobic mismatch $d_{\mathrm{P}} - d_{\mathrm{L}}^0$, for a membrane composed of (saturated) C_{14} chains. The asymptotic area per chain in these calculations is $a_0 \cong 32$ Å, corresponding to an area per head group of $2a_0 \cong 64$ Å^0 if the bilayer is regarded as composed of double-chain lipids. The hydrophobic thickness of the bilayer corresponding to this value of a_0 is $d_{\mathrm{L}}^0 \cong 24.5$ Å. The two curves shown in fig. 9b correspond to two different choices of the interfacial interaction parameters: $\gamma = 0.12kT/\text{Å}^2$, $a_{\mathrm{h}} = 20$ Å^2 and $\gamma = 0.08kT/\text{Å}^2$, $a_{\mathrm{h}} = 0$ (no head group repulsion); both choices yield $a_0 \cong 32$ Å^2 for the equilibrium head group area in the unperturbed bilayer.

The results show that ΔF is minimal around $d_{\mathrm{P}} - d_{\mathrm{L}}^0 \simeq 0$, yet $\Delta F > 0$ even if the hydrophobic thickness of the lipid and the protein match exactly. In the latter case ($d_{\mathrm{L}}^0 = d_{\mathrm{P}}$) the head group and surface tension components of ΔF are zero and, hence, ΔF is due entirely to chain distortion. The major contribution to ΔF in this case is

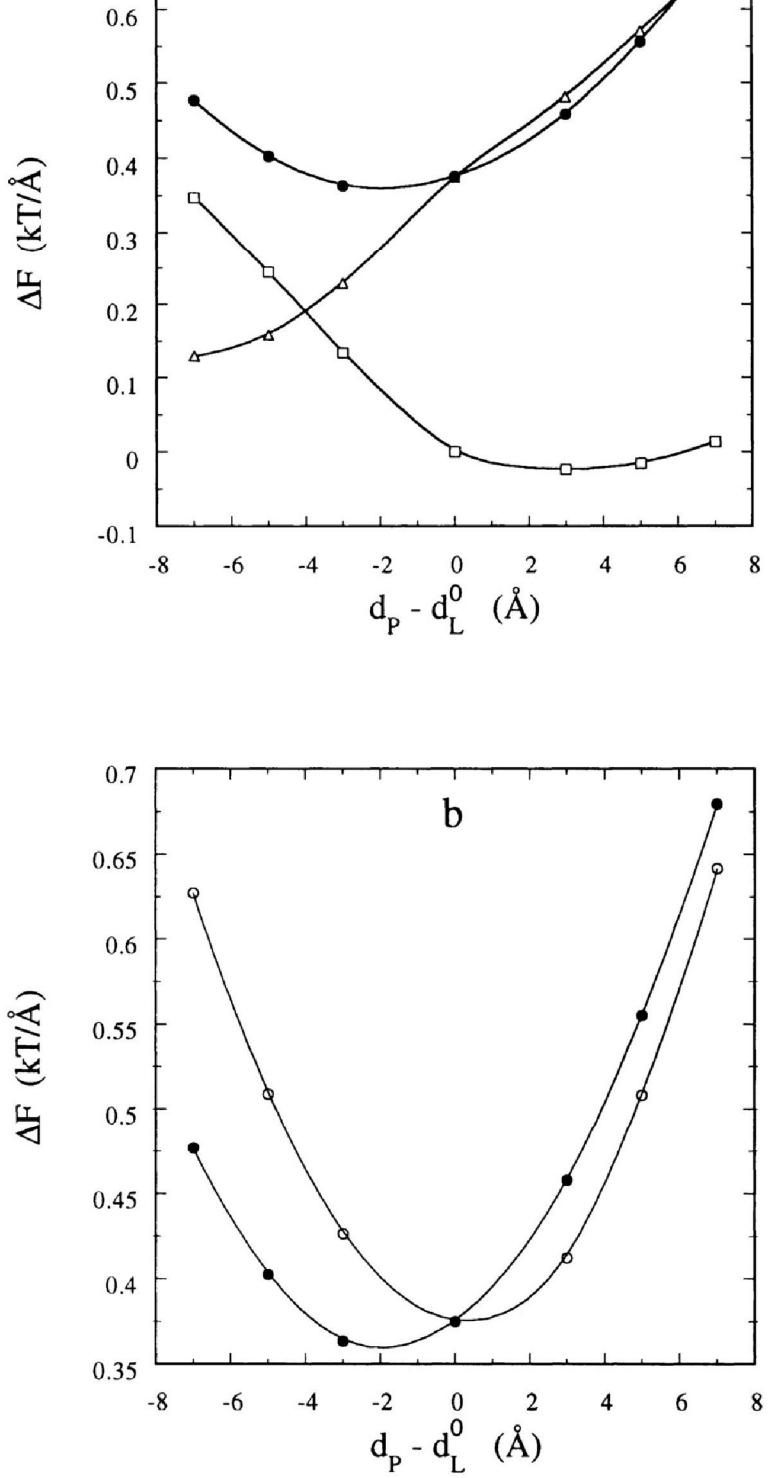

Fig. 9. a) The tail ($\Delta F_{\rm t}$, squares) and interfacial ($\Delta F_{\rm s} + \Delta F_{\rm h}$, triangles) contributions to the total lipid deformation free energy (solid circles), as a function of the hydrophobic mismatch [60]. The results correspond to the lipid-protein interaction free energy per unit length of the protein perimeter. The lipids are modeled as C_{14} chains with head group and surface interaction parameters: $\gamma = 0.12kT/\text{Å}^2$ and $a_{\rm h} = 20$ Å^2. The unperturbed bilayer thickness is $d_{\rm L}^0 = 24.5$ Å ($a_0 \simeq 32$ Å). b) The total lipid-protein interaction free energy (per 1 Å of protein perimeter) corresponding to the above case (solid circles), and to the case $\gamma = 0.08kT/\text{Å}^2$, $a_{\rm h} = 0$ (open circles). In both cases $d_{\rm L}^0 = 24.5$ Å.

chains in the immediate vicinity of the protein wall. This follows from the fact that many of the conformations α available to the chains in a protein free bilayer become forbidden once they are anchored near the protein; namely, all those conformations which 'penetrate' into the protein region. The lipid-protein interaction free energy for a system characterized by $d_{\rm L}^0 = d_{\rm P}$ has originally been studied by Marčelja [42]. The conclusions are similar.

A qualitative explanation for the increase of ΔF with the hydrophobic mismatch, $|d_{\rm P} - d_{\rm L}^0|$, is provided by the schematic illustration in fig. 8. When $d_{\rm P} > d_{\rm L}^0$ the chains in the vicinity of the protein are highly stretched, losing more of their conformational entropy, in addition to the loss implied by the presence of the wall. Thus, $\Delta F_{\rm t}(d_{\rm P} > d_{\rm L}^0) > \Delta F_{\rm t}(d_{\rm P} = d_{\rm L}^0)$. As the chains are stretched their average cross sectional area, $1/\sigma(x)$, decreases. However, since the interface is curved, the decrease in $a(x)$ and, consequently, the change in $\Delta F_{\rm h} + \Delta F_{\rm s}$ is marginal, see fig. 9a. Hence, for $d_{\rm P} > d_{\rm L}^0$, $\Delta F \simeq \Delta F_{\rm t} \simeq -T\Delta S_{\rm t}$ [60]. On the other hand, when $d_{\rm P} < d_{\rm L}^0$, the bilayer is compressed (in the vicinity of the protein), implying an increase in the average cross sectional area per chain ($1/\sigma(x) > 1/\sigma_0 = a_0$) and an even larger increase in the interfacial area per head group, $a(x) > 1/\sigma(x) > a_0$. Thus, the chains recover some of their lost conformational disorder: $\Delta F_{\rm t}(d_{\rm P} < d_{\rm L}^0) < \Delta F_{\rm t}(d_{\rm P} = d_{\rm L}^0)$. However, this gain in the tails free energy is generally over-compensated by the concomitant increase in the surface free energy $\Delta F_{\rm s}$. ($\Delta F_{\rm h}$ decreases, but to a considerably lesser extent. Note, though, that strong head group repulsion may shift the minimum of ΔF to a slightly negative $d_{\rm P} - d_{\rm L}^0$ value, as shown in fig. 9 by comparing the curves for $a_{\rm h} = 20$ Å^2 and $a_{\rm h} = 0$.) These trends are confirmed by the results shown in fig. 4 for the planar bilayer. Namely, when a increases beyond the equilibrium value a_0, the tail free energy decreases rather slowly, whereas the surface tension contribution increases linearly with a. Thus, for $d_{\rm L}^0 > d_{\rm P}$, the excess lipid-protein interaction free energy is due, mainly, to the increase in $\Delta F_{\rm s}$, see fig. 9a.

For all the data points shown in fig. 9 the value of ξ has been optimized by minimizing ΔF. It turns out that in all cases, the range of the perturbation ($\sim 3\xi$) is around 10–20 Å, corresponding to only a few molecular diameters. This result suggests that a microscopic, molecular, approach to the problem may be more appropriate than a phenomenological continuum theory.

In view of the relatively small number of lipid molecules affected by the presence of the protein, detailed molecular dynamics or Monte Carlo simulations of lipid-protein systems seem feasible. Considering the highly specific nature of lipid-protein interactions, simulation methods seem also to constitute the most appropriate approach to this problem. Only very few studies of this kind have so far been published [57, 59].

The model outlined in this section can be extended to bilayers containing a mixture of lipids, and to other shapes of hydrophobic proteins or other solutes. One interesting system which can be studied using the above methods is a lipid-cholesterol bilayer. On the other hand, as far as lipid-protein systems are concerned, it should be kept in mind that only few proteins can be regarded as simple, rigid, hydrophobic solutes. Furthermore, the model described above, like most previous models of lipid-protein

to other, more general and possibly more interesting, systems. In view of this fact, the model should be regarded as a small step towards understanding the intricacy of biological membranes.

5. Concluding remarks

Biological membranes, the subject matter of this volume, are extremely complex physico-chemical systems, not to mention their biological aspects. Even the 'model' amphiphilic bilayers, which have been considered here and which serve to mimic real membranes are also very complex many-body systems. In addition to their biological relevance, these systems are interesting and challenging theoretically, due to the special coupling between their microscopic and macroscopic behaviors and due to their self-organizing characteristics. Most of the relevant information on either biological or model membranes is, naturally, experimental. Nevertheless, the various theoretical models, ranging from highly qualitative phenomenological pictures to detailed molecular dynamics simulations also contribute to the understanding of their intricate nature. In this chapter we have outlined an intermediate approach to certain issues pertaining to lipid bilayers. Namely, a mean-field theory which takes into consideration some of the basic molecular interactions governing molecular organization in lipid bilayers but treating approximately the cooperative, thermodynamic, properties. As we have seen, the mean field approach is capable of predicting quite well certain single-chain properties (e.g., bond orientational order parameter profiles), as well as some thermodynamic-mechanical trends, e.g., the role of short chain amphiphiles in reducing the bending rigidity of bilayers.

Undoubtedly, in the near future computer simulations will become increasingly more detailed, reliable and efficient, and will yield relevant information on membrane structure and dynamics. However, computer simulations can not come up with the ultimate answers to all the interesting issues. For instance, it is hard to imagine, at least presently, a series of comprehensive molecular dynamics simulations of a mixed bilayer at different curvatures, performed in order to derive the bending modulus of the membrane. Also, in computer simulations one studies one set of parameters at a time. On the other hand, analytical theories, such as mean field models, often provide the explicit parameter dependence. Furthermore, mean field theories may also be useful in suggesting which parameters and conditions should be studied via simulation. Thus, there is still room and need for elaborating upon the existing approximate approaches. A major improvement towards this direction would be to treat, simultaneously, and on equal grounds the interactions governing chain organization within the hydrophobic region and the electrostatic and/or excluded volume forces prevailing at the membrane interface. As noted earlier, some work along this line has already been published and more work is in progress.

Acknowledgements

The molecular theory of chain packing statistics in amphiphilic aggregates reviewed in this chapter has been developed jointly with several collaborators: Igal Szleifer

Diego Kramer, Didier Roux and Sam Safran took part in the study of elastic constants. The analysis of lipid-solute interaction is a part of the Ph.D. Thesis of Debbie Fattal, who also performed some work on other issues mentioned in the text. I would also like to thank Erich Sackmann and Zhen-Gang Wang for many helpful and illuminating discussions, and Reinhard Lipowsky for his critical comments. The Yeshaya Horowitz Association, the Israel Science Foundation and the US–Israel Binational Science Foundation are acknowledged for financial support. The Fritz Haber Research Center, of which A.B.-S. is a member, is supported by the Minerva Gesellschaft für die Forschung, mbH, Munich, Germany.

References

1. Tanford, C., 1980, The Hydrophobic Effect, 2nd edition (Wiley, New York).
2. Ben-Naim, A., 1980, Hydrophobic Interactions (Plenum, New York).
3. Israelachvili, J.N., 1985, Intermolecular and Surface Forces (Academic Press, London).
4. Israelachvili, J.N., D.J. Mitchell and B.W. Ninham, 1976, Theory of self-assembly of hydrocarbon amphiphiles into micelles and bilayers, J. Chem. Soc. Faraday Trans. II **72**, 1525–1568.
5. Wennerström, H. and B. Lindman, 1979, Micelles, physical chemistry of surfactant association, Phys. Rep. **52**, 1–86.
6. Ben-Shaul, A. and W.M. Gelbart, 1994, Statistical thermodynamics of amphiphile self-assembly: Structure and phase transitions, in: Micelles, Membranes, Microemulsions and Monolayers, eds W.M. Gelbart, D. Roux and A. Ben-Shaul (Springer, New York) pp. 1–104.
7. Seelig, J. and W. Niederberger, 1974, Two pictures of a lipid bilayer. A comparison between deuterium label and spin-label experiments, Biochemistry **13**, 1585–1588.
8. Seelig, J. and A. Seelig, 1980, Lipid conformation in model membranes and biological membranes, Q. Rev. Biophys. **13**, 19–61.
9. Edholm, O., 1982, Order parameters in hydrocarbon chains, Chem. Phys. **65**, 259–270.
10. Jähnig, F., H. Vogel and L. Best, 1982, Unifying description of the effect of membrane proteins on lipid order. Verification for the melittin/dimyristoylphosphatidylcholine system, Biochemistry **21**, 6790–6798.
11. Nezil, F.A. and M. Bloom, 1992, Combined influence of cholesterol and synthetic amphiphilic peptides upon bilayer thickness in model membranes, Biophys. J. **61**, 1176–1183.
12. Lafleur, M., P.R. Cullis and M. Bloom, 1990, Modulation of the orientational order profile of the lipid acyl chain in the L_α phase, Eur., Biophys. J. **19**, 55–62.
13. Ipsen, J.H., O.G. Mouritsen and M. Bloom, 1990, Relationship between lipid membrane area, hydrophobic thickness and acyl-chain orientational order, Biophys. J. **57**, 405–412.
14. König, S., W. Pfeiffer, T. Bayerl, D. Richter and E. Sackmann, 1992, Molecular dynamics of lipid bilayers studied by incoherent quasi-elastic neutron scattering, J. Phys. II France **2**, 1589–1615.
15. Helfrich, W., 1973, Elastic properties of lipid bilayers: Theory and possible experiments, Z. Naturforsch. **28c**, 693–703.
16. Helfrich, W., 1974, Blocked lipid exchange in lipid bilayers and its possible influence on the shape of vesicles, Z. Naturforsch. **29c**, 510–515.
17. Helfrich, W., 1981, Amphiphilic mesophases made of defects, in: Les Houches Session XXXV "Physics of Defects", eds R. Balian et al. (North-Holland, Amsterdam) pp. 716–755.
18. Evans, E.A. and R. Skalak, 1979, Mechanics and thermodynamics of biomembranes, CRC Crit. Rev. Bioengineering, pp. 181–419.
19. Petrov, A.G. and I. Bivas, 1984, Elastic and flexoelectric aspects of out-of-plane fluctuations in biological and model membranes, Prog. Surf. Sci. **16**, 389–512.
20. Lipowsky, R., 1991, The conformation of membranes, Nature **349**, 475–481.
21. Porte, G., J. Appel, P. Bassereau and J. Marignian, 1989, L_α to L_3: A topology driven transition in phases of infinite fluid membranes, J. Phys. France **50**, 1335–1347.

optical microscopy to the determination of the curvature elastic modulus of biological and model membranes, J. Phys. France **48**, 855–867.
23. Faucon, J.F., M.D. Mitov, P. Melard, I. Bivas and P. Bothorel, 1989, Bending elasticity and thermal fluctuations of lipid membranes. Theoretical and experimental requirements, J. Phys. France **50**, 2389–2414.
24. Beblik, G., R.-M. Servuss and W. Helfrich, 1985, Bilayer bending rigidity of some synthetic lecithins, J. Phys. France **46**, 1773–1778.
25. Duwe, M.P., H. Engelhardt, H. Zilker and E. Sackmann, 1987, Curvature elasticity of smectic. A lipid bilayers and cell plasma membranes, Mol. Cryst. Liq. Cryst. **152**, 1–7.
26. Engelhardt, H., H.P. Duwe and E. Sackmann, 1985, Bilayer bending elasticity measured by Fourier analysis of thermally excited surface undulations of flaccid vesicles, J. Phys. Lett. France **46**, L395–L400.
27. Duwe, H.P., J. Kaes and E. Sackmann, 1990, Bending elastic moduli of lipid bilayers: Modulation by solutes, J. Phys. France **51**, 945–962.
28. Safinya, C.R., E.B. Sirota, D. Roux and G.S. Smith, 1989, Universality in interacting membranes: The effect of cosurfactant on the interfacial rigidity, Phys. Rev. Lett. **62**, 1134–1137.
29. di Meglio, J.-M., 1987, Phase diagram of lamellar phases: Rigidity and curvature, in: Physics of Amphiphilic Layers, Vol. 21, eds J. Meunier, D. Langevin and N. Boccara (Springer, Berlin) pp. 153–158.
30. Ben-Shaul, A., I. Szleifer and W.M. Gelbart, 1985, Chain organization and thermodynamics in micelles and bilayers, I. Theory, J. Chem. Phys. **83**, 3597–3611.
31. Szleifer, I., A. Ben-Shaul and W.M. Gelbart, 1985, Chain organization and thermodynamics in micelles and bilayers, II. Model calculations, J. Chem. Phys. **83**, 3612–3620.
32. Ben-Shaul, A. and W.M. Gelbart, 1985, Alkyl chain packing in micelles and bilayers, Annu. Rev. Phys. Chem. **36**, 179–211.
33. Ben-Shaul, A., I. Szleifer and W.M. Gelbart, 1984, Statistical thermodynamics of amphiphile chains in micelles, Proc. Nat. Acad. Sci. USA **81**, 4601–4605.
34. Szleifer, I., A. Ben-Shaul and W.M. Gelbart, 1986, Chain statistics in micelles: Effects of surface roughness and internal energy, J. Chem. Phys. **90**, 5277–5286.
35. Szleifer, I., A. Ben-Shaul and W.M. Gelbart, 1987, Statistical thermodynamics of molecular organization in mixed micelles and bilayers, J. Chem. Phys. **86**, 7094–7109.
36. Szleifer, I., D. Kramer, A. Ben-Shaul, D. Roux and W.M. Gelbart, 1988, Curvature elasticity of pure and mixed surfactant films, Phys. Rev. Lett. **60**, 1966–1969.
37. Szleifer, I., D. Kramer, A. Ben-Shaul, W.M. Gelbart and S.A. Safran, 1990, Molecular theory of curvature elasticity in surfactant films, J. Chem. Phys. **92**, 6800–6817.
38. Ben-Shaul, A., I. Szleifer and W.M. Gelbart, 1987, Molecular theory for amphiphile packing and elastic properties of monolayers and bilayers, in: Physics of Amphiphilic Layers, Springer Proceedings in Physics, Vol. 21, eds J. Meunier, D. Langevin and N. Boccara (Springer, Berlin) pp. 2–9.
39. Szleifer, I., A. Ben-Shaul and W.M. Gelbart, 1990, Chain packing statistics and thermodynamics of amphiphilic monolayers, J. Phys. Chem. **94**, 5081–5089.
40. Abney, J.R. and J.C. Owicki, 1985, Theories of protein-lipid and protein-protein interactions in membranes, in: Progress in Protein–Lipid Interactions, eds A. Watts and J.J.H.H.M. de Pont (Elsevier, Amsterdam) pp. 1–60.
41. Mouritsen, O.G. and M. Bloom, 1993, Models of lipid-protein interactions in membranes, Annu. Rev. Biophys. Biomol. Struct. **22**, 145–171.
42. Marčelja, S., 1976, Lipid-mediated protein interaction in membranes, Biochim. Biophys. Acta **455**, 1–7.
43. Owicki, J.C. and H.M. McConnell, 1979, Theory of protein-lipid and protein-protein interactions in bilayer membranes, Proc. Nat. Acad. Sci. USA **76**, 4750–4754.
44. Owicki, J.C., M.W. Springgate and H.M. McConnell, 1978, Theoretical study of protein-lipid interactions in bilayer membranes, Proc. Nat. Acad. Sci. USA **75**, 1616–1619.

345.
46. Peschke, J., J. Riegler and H. Möhwald, 1987, Quantitative analysis of membrane distortions induced by mismatch of protein and lipid hydrophobic thickness, Biophys. J. **14**, 385–391.
47. Kurrle, A., P. Rieber and E. Sackmann, 1990, Reconstitution of transferrin receptor in mixed lipid vesicles. An example of the role of elastic and electrostatic forces for protein/lipid assembly, Biochemistry **29**, 8274–8282.
48. Pink, D.A. and D. Chapman, 1979, Protein-lipid interactions in bilayer membranes: A lattice model, Proc. Nat. Acad. Sci. USA **76**, 1542–1546.
49. Mouritsen, O.G. and M. Bloom, 1984, Mattress model of lipid-protein interactions in membranes, Biophys. J. **46**, 141–153.
50. Sperotto, M.M. and O.G. Mouritsen, 1988, Dependence of lipid membrane phase transition temperature on the mismatch of protein and lipid hydrophobic thickness, Eur. Biophys. J. **16**, 1–10.
51. Sperotto, M.M. and O.G. Mouritsen, 1991, Mean-field and Monte Carlo simulation studies of the lateral distribution of proteins in membranes, Eur. Biophys. J. **19**, 157–168.
52. Elliott, J.R., D. Needham, J.P. Dilger and D.A. Haydon, 1983, The effects of bilayer thickness and tension on gramicidin single-channel lifetime, Biochim. Biophys. Acta **735**, 95–103.
53. Hladky, S.B. and D.A. Haydon, 1984, Ion movements in gramicidin channels, current topics in membranes and transport, Vol. 21, in: Ion Channels: Molecular and Physiological Aspects, Vol. 21, eds F. Bronner and W.D. Stein (Academic Press, New York) pp. 327–372.
54. Huang, H.W., 1986, Deformation free energy of bilayer membrane and its effects on gramicidin channel lifetiem, Biophys. J. **50**, 1061–1070.
55. Helfrich, P. and E. Jakobsson, 1990, Calculation of deformation energies and conformations in lipid membranes containing gramicidin channels, Biophys. J. **57**, 1075–1084.
56. Dan, N., P. Pincus and S.A. Safran, 1993, Membrane-induced interactions between inclusions, Langmuir **9**, 2768–2771.
57. Scott, H.L. and S.L. Cherng, 1978, Monte Carlo studies of phospholipid lamellae. Effects of proteins, cholesterol, bilayer curvature, and lateral mobility on order parameters, Biochim. Biophys. Acta **510**, 209–215.
58. Scott, H.L. and T.J. Coe, 1983, A theoretical study of lipid-protein interactions in bilayers, Biophys. J. **42**, 219–224.
59. Edholm, O. and J. Johansson, 1987, Lipid bilayer polypeptide interactions studied by molecular dynamics simulation, Eur. Biophys. J. **14**, 203–209.
60. Fattal, D. and A. Ben-Shaul, 1993, A molecular model for lipid-protein interaction in membranes: The role of hydrophobic mismatch, Biophys. J. **65**, 1795–1809.
61. Marčelja, S., 1974, Chain ordering in liquid crystals, II. Structure of bilayer membranes, Biochem. Biophys. Acta **367**, 165–176.
62. Jähnig, F., 1979, Molecular theory of lipid membrane order, J. Chem. Phys. **70**, 3279–3289.
63. Dill, K.A. and P.J. Flory, 1980, Interphases of chain molecules: Monolayers and lipid bilayer membranes, Proc. Nat. Acad. Sci. USA **77**, 3115–3119.
64. Dill, K.A. and P.J. Flory, 1981, Molecular organization in micelles and vesicles, Proc. Nat. Acad. Sci. USA **78**, 676–680.
65. Bivas, I. and A. Derzhanski, 1981, Statistical mechanical theory for hydrophobic core of lipid bilayer, Mol. Cryst. Liq. Cryst. **74**, 171–187.
66. Gruen, D.W.R., 1985, A model for the chains in amphiphilic aggregates, 1. Comparison with a molecular dynamics simulation of a bilayer, J. Phys. Chem. **89**, 146–153. 2. Thermodynamics and experimental comparisons for aggregates of different shape and size, J. Phys. Chem. **89**, 153–163.
67. Dill, K.A., J. Naghizadeh and J.A. Marqusee, 1988, Chain molecules at high densities at interfaces, Annu. Rev. Phys. Chem. **39**, 425–462.
68. Leermakers, F.A.M. and J.M.H.M. Scheutjens, 1989, Statistical thermodynamics of association colloids, 1. Lipid bilayers, J. Chem. Phys. **89**, 3264–3274. 3. The gel to liquid phase transition of lipid membranes, J. Chem. Phys. **89**, 6912–6924.

colloids, 2. Lipid vesicles, J. Phys. Chem. **93**, 7417–7426.
70. Egberts, E. and H.J.C. Berendsen, 1988, Molecular dynamics simulation of a smectic liquid crystal with atomic detail, J. Phys. Chem. **89**, 3718–3732.
71. van der Ploeg, P. and H.J.C. Berendsen, 1983, Molecular dynamics of a bilayer membrane, Mol. Phys. **49**, 233–248.
72. Edholm, O., H.J.C. Berendsen and P. van der Ploeg, 1983, Conformational entropy of a bilayer membrane derived from a molecular dynamics simulation, Mol. Phys. **48**, 379–388.
73. Biswas, A. and B.L. Schurman, 1991, Molecular dynamics simulation of a dense model bilayer of chain molecules with fixed head groups, J. Chem. Phys. **95**, 5377–5386.
74. Pastor, R.W., R.M. Venable and M. Karplus, 1988, Brownian dynamics simulations of a lipid chain in a membrane bilayer, J. Chem. Phys. **89**, 1112–1127.
75. Milik, M., A. Kolinski and J. Skolnik, 1990, Monte Carlo dynamics of a dense system of chain molecules constrained to lie near an interface. A simplified membrane model, J. Chem. Phys. **93**, 4440–4446.
76. Heller, H., M. Schaefer and K. Schulten, 1993, Molecular dynamics simulation of a bilayer of 200 lipids in the gel and in the liquid crystal phase, J. Phys. Chem. **97**, 8343–8360.
77. Andelman, D., 1994, Electrostatic properties of membranes, *see* This volume.
78. Jönsson, B. and H. Wennerström, 1981, Thermodynamics of ionic amphiphile-water systems, J. Colloid Interface Sci. **80**, 482–496.
79. Dill, K.A. and D. Stigter, 1988, Lateral interactions among phosphatidylcholine and phosphatidylethanolamine head groups in phospholipid monolayers and bilayers, Biochemistry **27**, 3446–3453.
80. Stigter, D. and K.A. Dill, 1988, Lateral interactions among phospholipid head groups at the heptane/water interface, Langmuir **4**, 200–209.
81. Winterhalter, M. and W. Helfrich, 1992, Bending elasticity of electrically charged bilayers: Coupled monolayers, neutral surfaces, and balancing stresses, J. Phys. Chem. **96**, 327–330.
82. Mitchell, D.J. and B.W. Ninham, 1989, Curvature elasticity of charged membranes, Langmuir **5**, 1121–1123.
83. Lekkerkerker, H.N.W., 1989, Contribution of the electric double layer to the curvature elasticity of charged amphiphilic monolayers, Physica **A159**, 319–328.
84. Ennis, J., 1992, Spontaneous curvature of surfactant films, J. Chem. Phys. **97**, 663–678.
85. May, S., 1992, Krummungselastizität ionischer Monoschichten, Diplomarbeit, Friedrich-Schiller-Universität, Jena.
86. Naor, A., S. Puvvada and D. Blankschtein, 1992, An analytical expression for the free energy of micellization, J. Phys. Chem. **96**, 7830–7832.
87. Flory, P.J., 1969, Statistical mechanics of chain molecules (Wiley, New York).
88. Carignano, M.A. and I. Szleifer, 1993, Statistical theory of grafted polymer layers, J. Chem. Phys. **98**, 5006–5009.
89. Hladky, S.B. and D.W.R. Gruen, 1982, Thickness fluctuations in black lipid membranes, Biophys. J. **38**, 251–258.
90. Lewis, B.A. and D.M. Engelman, 1983, Lipid bilayer thickness varies linearly with acyl chain length in fluid phosphatidylcholine vesicles, J. Mol. Biol. **166**, 211–217.
91. deGennes, P.G., 1979, Scaling Concepts in Polymer Physics (Cornell Univ. Press, Ithaca).
92. Wang, Z.-G. and S.A. Safran, 1991, Curvature elasticity of diblock copolymer monolayers, J. Chem. Phys. **94**, 679–687.
93. Wang, Z.-G., 1992, Curvature instability of diblock copolymer bilayers, Macromolecules **25**, 3702–3705.
94. Wang, Z.-G. and S.A. Safran, 1990, Curvature elasticity of ordered bicontinuous phases, Europhys. Lett. **11**, 425–430.
95. Kozlov, M.M. and M. Winterhalter, 1991, Elastic moduli for strongly curved monolayers. Position of the neutral surface, J. Phys. II France **1**, 1077–1084.
96. Helfrich, W. and H.M. Kozlov, 1993, Bending tensions and the rigidity of fluid membranes, J. Phys. II France **3**, 287–292.

France **49**, 1951–1962.
98. Cantor, R.S., 1993, Statistical thermodynamics of curvature elasticity in surfactant monolayer films: A molecular approach, J. Chem. Phys. **99**, 7124–7149.
99. Gelbart, W.M. and A. Ben-Shaul, 1987, Chain packing and compressional elasticity of surfactant films, in: Physics of Amphiphilic Layers. Springer Proceedings in Physics, Vol. 21, eds J. Meunier, D. Langevin and N. Boccara (Springer, Berlin) pp. 9–12.
100. Bloom, M., E. Evans and O.G. Mouritsen, 1991, Physical properties of the fluid lipid-bilayer component of cell membranes: A perspective, Q. Rev. Biophys. **24**, 293–397.
101. Sackmann, E., S. Sen-fang, K. Wirthensohn and T. Urumow, 1987, Lipid-protein interaction: Selectivity and receptor binding, in: Biomembrane and Receptor Mechanics. Fidia Research Series 7, eds E. Bertoli, D. Chapman, A. Cambria and U. Scapagini.
102. Sackmann, E., 1990, Molecular and global structure and dynamics of membranes and lipid bilayers, Can. J. Phys. **68**, 999–1012.